Characterizing the Effect of Simultaneous Enhancements of Reducing Gas Species on Figaro Taguchi Gas Sensor Resistance Response

Adil Shah, Olivier Laurent, Grégoire Broquet, Pramod Kumar, Philippe Ciais

ACS OMEGA

Open Access

http://pubs.acs.org/journal/acsodf

Article

Characterizing the Effect of Simultaneous Enhancements of Reducing Gas Species on Figaro Taguchi Gas Sensor Resistance Response

Adil Shah,* Olivier Laurent, Grégoire Broquet, Pramod Kumar, and Philippe Ciais

Cite This: https://doi.org/10.1021/acsomega.4c06397

Read Online

ACCESS | Metrics & More | Article Recommendations | Supporting Information

ABSTRACT: The resistance of the Figaro Taguchi Gas Sensor (TGS) decreases when exposed to reducing gas enhancements. TGS gas response can be characterized by comparing measured resistance to a reference resistance, representative of sampling in identical environmental conditions but with no reducing gas enhancement. Thus, this resistance ratio (RR) allows for characterization of reducing gas response, independent of other environmental effects. This work presents controlled laboratory experiments, measurements, and modeling for an analysis on the effect of reducing gas cross-sensitivities on RR. The methane mole fraction ($[CH_4]$) was raised to approximately 9 ppm from a 0.492 ppm reference level, and carbon monoxide mole fraction ([CO]) was raised to approximately 4 ppm from a 0 ppm reference level, through multiple simultaneous steps. The independent effect of each gas on RR was directly multiplied, resulting in an inferior RR compared with measurements, implying an interdependence effect. For example, for one TGS unit, when deriving $[CH_4]$ from RR, a 6 ppm $[CH_4]$ measurement would be underestimated by 6% at 1 ppm [CO], but only by 1.6% at 0.1 ppm [CO]. A key implication of residual interdependence effects is that any gas characterization must be conducted with the same reference levels of each other reducing gas expected during field deployment, even if measuring a single gas. A first-order interdependence correction is proposed to account for such interdependence effects. Yet, each TGS behaves differently, and interdependence testing takes time. Therefore, the TGS best serves to detect single reducing gases, assuming all other reducing gases to remain constant at their reference levels.

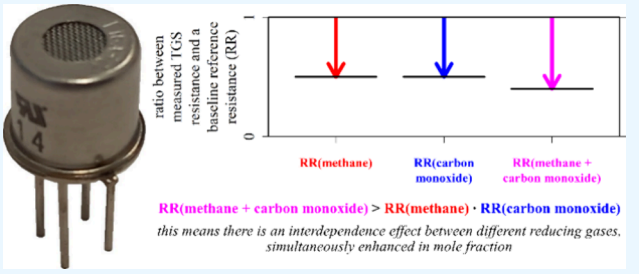

1. INTRODUCTION

Semiconductor-based metal oxide (SMO) materials can be used as gas sensors[1] when activated under a potential difference,[2,3] with n-type SMO sensors sensitive to reducing gases.[4] Atmospheric oxygen adsorbs onto n-type SMO surfaces, causing the extraction of electrons from the bulk material, thereby initially raising resistance.[5] Reducing gases readily oxidize upon reaction with this activated oxygen layer, causing resistance decrease.[6,7] Thus, a net increase in reducing gas exposure causes a net SMO resistance drop. However, a fundamental challenge is converting measured SMO resistance into a specific reducing gas mole fraction,[7−12] where mole fraction is defined as the number of molecules of a certain gas compared to the total number of gas molecules in a defined volume.[13] Deriving mole fractions is further complicated by other environmental factors such as ambient temperature and water mole fraction ($[H_2O]$), which can also affect SMO resistance.[2,3,14−17] It is vitally important to understand the response of SMO sensors to various gas mixtures prior to sensor deployment.

We characterized the Figaro Taguchi Gas Senor (TGS) 2611-C00 and TGS 2611-E00 manufactured by Figaro Engineering Inc. (Mino, Osaka, Japan). These grain-based sensors[6,18] measure various reducing gases, including methane up to high (percentage) levels.[19,20] The TGS is cheap (less than 10^2 €), is commercially available,[9] and can operate in wet air.[21,22] In contrast, many SMO sensors function optimally in dry conditions.[8,23] TGS resistance (R) has been combined with environmental measurements in a variety of methods to derive reducing gas mole fractions, including deterministic models[24−27] and machine learning approaches.[22,28−30] However, cross-sensitivities between reducing gases including methane, carbon monoxide, ethane, and hydrogen sulfide[6,12,31,32] may cause complications in deriving mole fractions of a single gas; such effects must be understood and characterized.

Reducing gas mole fractions can be derived from the resistance ratio (RR) between measured TGS resistance when exposed to a certain gas mixture, compared to a baseline reference resistance (R_0) derived in a reference gas

Received: July 10, 2024
Revised: October 8, 2024
Accepted: October 16, 2024

mixture;[3,6,33] all reducing gases are defined to be at reference mole fraction levels in the reference gas. RR is defined here with R_0 as the RR denominator. While the reference gas is typically ambient air-based,[3] any gas blend can be used for R_0, provided that (noncharacterized) reducing gas mole fractions remain invariant.[32] This R_0 is measured in identical conditions as those of measured TGS resistance during sampling (with the exception of reference levels of characterized reducing gas mole fractions). R_0 can vary for numerous reasons but can be modeled over time as a function of environmental conditions (excluding characterized reducing gas mole fractions), principally [H_2O] and ambient temperature.[32] An RR cancels the effect of these environmental conditions, allowing for the independent analysis of the effect of reducing gases during sampling.[3] Jørgensen et al.[33] showed this for methane, observing similar RR curves in different environmental conditions, by raising the methane mole fraction ([CH_4]) from 0 ppm (where ppm is parts per million) up to 100 ppm. Using RRs is recommended by the sensor manufacturer, albeit to derive high mole fractions.[19,20] RRs have previously been employed for single reducing gas measurements, assuming all other reducing gases being fixed at their reference levels,[32,33] absolving the requirement to consider cross-sensitivities.

Clifford and Tuma[6] converted RR into single gas mole fractions with an adapted power fit. Shah et al.[34] proposed a similar model, including a reference mole fraction term. This sets the RR to one at reference mole fraction levels (i.e., measured TGS resistance being equal to R_0); the RR decreases with increasing reducing gas mole fraction, such that the RR tends to zero at an infinite mole fraction. Although only individual reducing gases (methane, carbon monoxide, and hydrogen sulfide) have been tested,[32] it is proposed that a combined multiplicative model (CMM) may incorporate the effect of multiple reducing gases, treating each gas as an independent multiplicative contributor toward net RR.[34] This relies on each reducing gas reacting competitively with activated oxygen atoms on the SMO surface but for reducing gases not to interact with each other. The initial presence of one reducing gas results in a lower starting resistance, serving as a new (lower) R_0 for a secondary reducing gas to follow the original model. This proposed behavior means that, for example, if one gas causes an RR of 0.5 and another gas also causes an RR of 0.5, the combined effect of the two gases is a net RR of 0.25 (i.e., starting R_0 reduces by 75%).

The Shah et al.[34] approach was tested to derive [CH_4] at a landfill site using the TGS 2611-C00 and TGS 2611-E00, assuming stable and constant levels of all other reducing gases (including carbon monoxide that influences both TGSs).[32] This is a reasonable assumption, with methane being the main reducing gas emitted from landfill.[35] However, in complex locations with simultaneous variability in multiple reducing gases (simultaneously enhanced in mole fraction), the proposed Shah et al.[34] multiple-gas CMM must be reliably tested to account for cross-sensitivities.[12] Adequate sensor testing underpins the accuracy of any mole fraction measurements. Taking methane, for example, it may be coemitted with other gases, for instance ethane at gas extraction sites[36] or carbon monoxide due to fires (pyrogenic methane emissions) within boreal wetlands;[17] these complex examples both require a reliable TGS CMM.

An improved understanding of existing technologies, such as TGSs, is essential for their use during reducing gas sampling. In this study, we characterized the effect of [CH_4] and carbon monoxide mole fraction ([CO]) enhancements (compared to reference levels) on RR, with an overall objective of deriving [CH_4]. This work aims to build a more general understanding of the effect of variations in multiple gas mole fractions on TGS resistance measurements. Additional reducing gases were not simultaneously tested here, as this is beyond the scope of this study, although this would be welcome in future work. Methane and carbon monoxide were specifically tested as they both interact with the TGS 2611-C00 and two TGS 2611-E00. Section 2 describes the laboratory testing procedure used to sample various [CH_4] and [CO] gas blends under controlled conditions. Independent [CH_4] and [CO] model fitting coefficients are derived and tested when applied to each gas mole fraction combination in Section 3. We also propose an improvement to the original Shah et al.[34] CMM for multiple reducing gases in Section 3, extending the model by correcting for previously unaccounted interdependence effects. This provides a significant improvement in RR estimation compared with the original CMM approach. Although only two specific gases were tested here, the conclusions of this work may, in theory, be applied to any pair of reducing gases with an interdependence effect. In Section 4, we discuss the implications of our findings on future TGS gas characterization work and the significance of any model disparity. We summarize our outcomes in Section 5.

2. EXPERIMENTAL DESCRIPTION

2.2. Laboratory Testing. A TGS 2611-C00 and two TGS 2611-E00 units from different production batches (labeled TGS 2611-E00 A and TGS 2611-E00 B) were simultaneously tested in a logging system, described in Section S1 in the Supporting Information, which also contained a temperature sensor. The overall laboratory testing principle was to characterize RR, while sampling various [CH_4] and [CO] combinations. An R_0 for each TGS may ordinarily be characterized as a function of non-gas mole fraction environmental conditions such as temperature and [H_2O], while sampling a constant reference gas containing reference levels of all reducing gases.[32] However, deriving such a model requires extensive laboratory testing in a multitude of temperature and [H_2O] combinations. As R_0 modeling is not the focus of this work, an empirical R_0 can instead be derived in stable environmental conditions. A fit can be applied to regular reference gas sampling intervals as a function of time to account for natural sensor drift or minor environmental variability. This approach requires a sufficient number of reference sampling intervals and changes in environmental conditions to be sufficiently small, so that they incorporate into the RR fit as a function of time. With these objectives in mind, various [CH_4] and [CO] enhancement combinations were sampled between reference gas sampling periods, while minimizing environmental variability (including [H_2O] and temperature). Only a single set of environmental conditions was tested (as required here), with previous research[33] showing RR gas response to be independent of such conditions. Thus, the broad conclusions from this work can be applied in other conditions, as RRs are independent of the environment in which they are derived.

[CH_4] and [CO] gas blends were obtained using mass-flow controllers (Bronkhorst High-Tech B.V., AK Ruurlo, The Netherlands), which controlled the flow from various gas cylinders, while maintaining a fixed net 1.5 dm^3 flow rate (at 101 325 Pa and 273.15 K) to the logging cell; this fixed flow

https://doi.org/10.1021/acsomega.4c06397
ACS Omega XXXX, XXX, XXX−XXX

rate ensures a constant TGS air flow cooling effect. To maximize [H_2O] stability, all gas passed through a dew-point generator (LI-610, LI-COR, Inc., Lincoln, Nebraska, USA) with a fixed 8 °C dew-point setting. Air humidification is essential as the TGS can yield abnormal measurements in dry conditions.[18,21,29] In addition, small [H_2O] changes can result in a prolonged and residual TGS resistance response.[34] Hence, this dew-point was sampled for at least 24 h before testing.

A high-precision reference gas analyzer (Picarro G2401, Picarro, Inc., Santa Clara, California, USA) sampled downstream of the TGS cell, with a maximum sampling frequency of 0.3 Hz. It measures [CH_4], [CO], and [H_2O] with a 0.2 Hz manufacturer-rated precision of better than ±0.001, ±0.015, and ±30 ppm, respectively.[37] A laboratory-derived water correction was applied to all raw wet methane mole fraction measurements to correct for dilution effects, spectral overlap, and spectral peak broadening. A simple offset correction was applied to all raw dry carbon monoxide mole fraction measurements by subtracting the average measured mole fraction from periods corresponding to sampling a [CO] of 0 ppm. A time correction was applied to align the reference instrument time stamp with that of the TGS logger. In addition, all reference analyzer measurements were interpolated to the higher 1 Hz TGS time stamp. All mole fraction measurements presented henceforth are dry mole fractions, and thus, the subsequent TGS characterization analysis is based on dry [CH_4] and [CO].

Gas from three synthetic gas cylinders (Deuste Gas Solutions GmbH, Schömberg, Germany) was combined up to maximum targeted levels of 9 ppm of [CH_4] and 4 ppm of [CO]. Cylinder 1 is a zero-air cylinder containing gas with trace [CH_4] and [CO] levels (where trace levels refer to minor residual contaminant gas levels). Cylinder 2 contains gas with a [CH_4] of 202 ppm and trace [CO] levels. Cylinder 3 contains gas with trace [CH_4] levels and a [CO] of 5 ppm. All cylinder 1 and cylinder 2 gas passed through a carbon monoxide chemical scrubber (Sofnocat 514, Molecular Products, Limited, Harlow, Essex, UK). Each synthetic gas cylinder contains a residual nitrogen, oxygen, and argon natural balance. It is important to note that TGS RR gas models derived using synthetic air cylinders cannot be applied to ambient air sampling, as previous research has shown such model coefficients to be invalid in ambient conditions.[6,32−34,38] This is not an issue in this TGS characterization study evaluating the general nature of gas response in laboratory settings, which considers the same synthetic standard reference gas throughout the forthcoming analysis.

In this specific interdependence study, the reference methane mole fraction ($[CH_4]_0$) and reference carbon monoxide mole fraction ($[CO]_0$) were minimized for heightened TGS sensitivity. This maximizes TGS response to mole fraction enhancements,[6] thus improving RR characterization. $[CO]_0$ was simply set to 0 ppm, which could be reliably achieved by using the carbon monoxide chemical scrubber. However, a 0.5 ppm $[CH_4]_0$ setting was instead targeted, as removing residual methane is complex, therefore making it easier to reliably raise $[CH_4]_0$ to a predetermined nonzero level. This reference gas was sampled for at least 2 h at the start of the test. Then, each testing gas mixture was sampled for 30 min, before again sampling the reference gas for 30 min. A 30 min duration was deemed to be sufficient to allow the sensors to stabilize to exposure to each gas mixture. This process was repeated to sample 30 different testing gas blends, as illustrated in Figure 1. It was initially planned to sample each combination of seven different [CH_4] levels up to

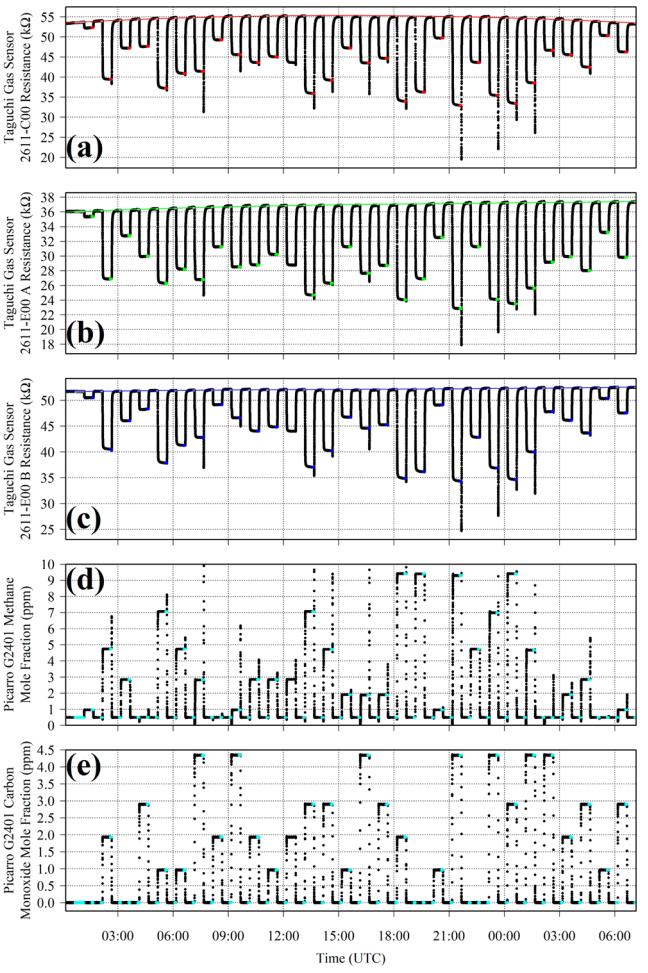

Figure 1. (a) TGS 2611-C00 resistance, (b) TGS 2611-E00 A resistance, (c) TGS 2611-C00 resistance, (d) reference gas analyzer [CH_4], and (e) reference gas analyzer [CO] measurements, all plotted as black dots. 5 min averaging periods for testing gas combinations are plotted on top as colored dots in (a), (b), and (c). 5 min R_0 derivation periods for each TGS are shown as white-highlighted dots in (a), (b), and (c), over which corresponding polynomial fits are plotted as colored lines. All 5 min R_0 derivation periods and averaging periods for testing gas combinations are plotted on top as cyan dots in (d) and (e).

roughly 9 ppm and five different [CO] levels up to roughly 4 ppm (35 combinations in total) in a random order (to avoid temporal bias), representing a sufficient number of gas blends across a large enough range to characterize TGS interdependence. Unfortunately, this was not achieved as the dew-point generator ran dry and one gas mixture was accidentally sampled twice, which has been omitted from the subsequent analysis. Nevertheless, 29 unique [CH_4] and [CO] combinations were tested, representing a sufficiently large data set to satisfy the objectives of this work.

Ambient temperature and [H_2O] were kept as stable as possible. The dew-point generator maintained a stable [H_2O] with an average and (standard deviation) variability of (10 703 ± 21) ppm during testing. The testing duration is defined as from 60 min before the first gas combination sampling period up to 30 min after the end of the final gas combination

https://doi.org/10.1021/acsomega.4c06397
ACS Omega XXXX, XXX, XXX−XXX

Table 1. Derived Eq 1 m and μ Coefficients for Methane, for Each TGS, with the RMSE in RR and the R^2 for Each Fit Also Given[a]

sensor	m (ppm)	μ	RMSE (mΩ Ω^{-1})	R^2	RR change from 0.492 to 1.492 ppm [CH_4] (Ω Ω^{-1})
TGS 2611-C00	10.9 ± 0.7	0.70 ± 0.04	±0.945	0.999933	−0.0601
TGS 2611-E00 A	13.3 ± 0.5	0.63 ± 0.02	±0.386	0.999983	−0.0447
TGS 2611-E00 B	12.2 ± 0.5	0.67 ± 0.02	±0.567	0.999970	−0.0514

[a]The RR change for a 1 ppm of [CH_4] increase from $[CH_4]_0$ (with [CO] equal to $[CO]_0$) is provided.

Table 2. Derived Eq 1 m and μ Coefficients for Methane, for Each TGS, with the RMSE in RR and the R^2 for Each Fit Also Given[a]

sensor	n (ppm)	ν	RMSE (mΩ Ω^{-1})	R^2	RR change from 0.0 to 0.1 ppm [CO] (Ω Ω^{-1})
TGS 2611-C00	0.6 ± 0.2	0.074 ± 0.010	±2.93	0.990	−0.0114
TGS 2611-E00 A	0.5 ± 0.2	0.107 ± 0.018	±5.47	0.980	−0.0186
TGS 2611-E00 B	0.7 ± 0.3	0.046 ± 0.010	±2.72	0.975	−0.0058

[a]The RR change for a 0.1 ppm [CO] increase from $[CO]_0$ (with [CH_4] equal to $[CH_4]_0$) is provided.

sampling period, corresponding to 31 h of total testing. All testing was conducted in an air-conditioned laboratory. This resulted in an average ambient temperature and (standard deviation) variability of (307.3 ± 0.3) K, as measured by the temperature sensor inside the TGS cell.

3. ANALYSIS AND RESULTS

3.1. Data Preparation. For the subsequent analysis, TGS 2611-C00, TGS 2611-E00 A, and TGS 2611-E00 B measurements were first converted into the ratio between the average measured TGS resistance and a corresponding R_0 value, for each [CH_4] and [CO] testing combination. The average measured TGS resistance is the numerator within RR, and the corresponding R_0 is the denominator. Figure 1 shows variability in R_0 levels between each TGS, despite the fact that they all sampled an identical reference gas (see the white-highlighted dots). This disparity is because each TGS has unique properties and comes from different batches. In addition, each TGS had a different position within the sampling cell that led to slightly different heating and cooling effects. Furthermore, each TGS was of different age and was thus exposed to different gases that could impair sensor performance over time. Yet, all of these issues are irrelevant when using sensor-specific R_0 values to derive RRs, which are independent of environmental conditions.[33] Thus, R_0 was derived for each TGS, which was modeled as a function of time from available reference sampling. To achieve this, a third-order polynomial fit was applied to 30 min of reference sampling at start of the experiment and 5 min of sampling from the end of each 30 min reference gas sampling interval, as a function of time (colored lines in Figure 1a−c). This 5 min average was used as 25 min permitted a sufficient TGS stabilization time after sampling the previous gas mixture, while a 5 min averaging duration was deemed to be sufficient to account for short-term drift and noise. [CH_4] was on average (0.492 ± 0.001) ppm during these periods, according to the reference gas analyzer, thus serving as $[CH_4]_0$ in the subsequent analysis. This yielded modeled R_0 values corresponding to each measured TGS resistance data point. Then, a 5 min average in measured TGS resistance was taken from the end of each successful 30 min testing gas sampling interval (colored dots in Figure 1a−c), alongside a corresponding average modeled R_0. The ratio between these two averages was taken for each gas combination. Corresponding [CH_4] and [CO] 5 min averages were also taken from the reference gas analyzer.

3.2. Individual Model Fits. TGS RRs were first used to derive individual gas characterization fits. Shah et al.[32] showed that [CH_4] can be related to RR through

$$R = R_0 \times \left(1 + \left(\frac{[CH_4] - [CH_4]_0}{m}\right)\right)^{-\mu} \quad (1)$$

assuming all other reducing gases at their reference levels. Clifford and Tuma[6] applied a similar RR model to [CH_4], although without a $[CH_4]_0$ term. The characteristic methane mole fraction (m) and the methane power (μ) in eq 1 were derived for each TGS by fitting all four RRs against corresponding 5 min average [CH_4] values, where [CO] was equal to $[CO]_0$, with $[CH_4]_0$ set to 0.492 ppm (see Table 1 for values). Shah et al.[32] also showed that an analogous fit for [CO] can be related to RR through

$$R = R_0 \times \left(1 + \left(\frac{[CO] - [CO]_0}{n}\right)\right)^{-\nu} \quad (2)$$

assuming all other reducing gases at their reference levels. The characteristic carbon monoxide mole fraction (n) and the carbon monoxide power (ν) in eq 2 were derived for each TGS by fitting all four RRs against corresponding 5 min average [CO] values, where [CH_4] was equal to $[CH_4]_0$, with $[CO]_0$ set to 0 ppm (see Table 2 for values).

For both fits, a nonlinear least-squares (NLS) regression was applied between RR and mole fraction (see Figure 2 for regression fits). All NLS regression analyses in this manuscript were computed using the "nls" function of R version 4.2.2.[39] The root-mean-square error (RMSE) in RR is also given in Tables 1 and 2 alongside the coefficient of determination (R^2) of each fit. Standard deviation uncertainty values are given for m, μ, n, and ν, which were provided by R version 4.2.2[39] using rescaled covariances based on Hessian matrices. As discussed in Section 2, despite the fact that this test was conducted in specific fixed environmental conditions, an RR analysis is independent of such conditions and the same RR fit can be expected in different conditions, as observed elsewhere.[33] These fits can therefore be used to understand the general TGS response to multiple reducing gas enhancements, regardless of variability in other environmental conditions.

Figure 2 shows that good RR fits were derived as a function of both [CH_4] and [CO] individually. It is important to note

https://doi.org/10.1021/acsomega.4c06397
ACS Omega XXXX, XXX, XXX−XXX

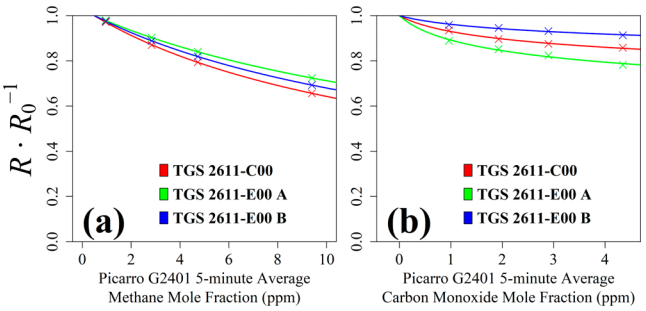

Figure 2. 5 min average (a) $[CH_4]$ measurements and (b) [CO] measurements made by the reference gas analyzer, plotted against corresponding TGS RRs as colored crosses for the three tested sensors (see legend for TGS colors). Corresponding eq 1 and 2 model fits are plotted as colored lines in (a) and (b), respectively.

here that, in general, when evaluating the quality of such a fit, the reference mole fraction (i.e., $[CH_4]_0$ and $[CO]_0$) must be considered as well as the enhancement range above this level, which should both reflect final sampling conditions. Although larger mole fraction ranges may extend the eq 1 or 2 fit, this has no added value in this gas combination study, with the same $[CH_4]$ and [CO] testing ranges used in the forthcoming analysis. With these caveats in mind, Figure 2 shows the $[CH_4]$ fit to be better than the [CO] fit, with the RR variation in this study being far larger across the tested $[CH_4]$ range than the [CO] range. Thus, Table 1 RMSE and R^2 values are better for $[CH_4]$ than corresponding Table 2 values for [CO]. For example, the RR RMSE for TGS 2611-C00 for the $[CH_4]$ fit is almost a third of that for the [CO] fit. Yet, an R^2 of at least 0.9 for all fits for each TGS implies that all six fits are adequate for the forthcoming analysis, especially considering that each fit was derived from only four data points.

3.3. Combined Multiplicative Model Testing. Shah et al.[34] proposed that the RR effect of multiple reducing gases can be combined multiplicatively for each reducing gas (g) in each testing gas mixture following

$$R = R_0 \times \prod_g \left(1 + \left(\frac{[M_g] - [M_g]_0}{c_g}\right)\right)^{-\gamma_g} \quad (3)$$

as given by Shah et al.[32] The capital Greek letter "pi" represents a product of a sequence in the same way that the capital Greek letter "sigma" represents a summation. $[M_g]$ is the mole fraction of g, $[M_g]_0$ is the mole fraction of g in the reference gas, c_g is the characteristic mole fraction of g, and γ_g is the power of g. A similar CMM was proposed by Clifford and Tuma[6] for the TGS 812, but instead used a single fixed power (or integer orders of this power) for all gases. The general CMM presented here effectively assumes that the effect of each individual reducing gas on RR can be multiplied together to model the net resistance decrease from the starting R_0. Although $[H_2O]$ may be included with the CMM,[6] this is not required in the Shah et al.[34] CMM as $[H_2O]$ is already incorporated into R_0, meaning that it cancels out in an RR and is therefore not treated as a reducing gas, contributing toward net RR.

For the specific case of $[CH_4]$ and [CO] variations, eq 3 can be expressed as

$$R = R_0 \times \left(1 + \left(\frac{[CH_4] - [CH_4]_0}{m}\right)\right)^{-\mu} \times \left(1 + \left(\frac{[CO] - [CO]_0}{n}\right)\right)^{-\nu} \quad (4)$$

which assumes net RR to be a product of a methane term and a carbon monoxide term. This also assumes all other reducing gas mole fractions to be constant. When [CO] equals $[CO]_0$, eq 4 simplifies to eq 1 and when $[CH_4]$ equals $[CO]_0$, eq 4 simplifies to eq 2, as expected. If any additional reducing gases were simultaneously tested in this work, they could simply be included as additional multiplicative terms within eq 4, according to eq 3.

Equation 4 could be tested with m, μ, n, and ν for each TGS (see Tables 1 and 2), as a function of corresponding 5 min averaged $[CH_4]$ and [CO] from the reference gas analyzer. This therefore tests the validity of the original Shah et al.[34] CMM with reducing gas enhancement combinations ($[CH_4]$ and [CO] enhancements in this study) for the first time. Each observed 5 min average RR was compared to RR predicted using eq 4 in Figure 3. The RMSE between observed and corresponding predicted RRs is provided in Table 3, along with the Pearson correlation coefficient and mean bias. For general reference, RRs fall between 0 and 1 $\Omega\ \Omega^{-1}$, assuming reducing gas mole fractions to either equal or exceed their reference levels. The significance of an RR change can also be gauged considering a mole fraction change. The effect of a 1 ppm $[CH_4]$ enhancement compared to $[CH_4]_0$ and the effect of a 0.1 ppm [CO] enhancement compared to $[CO]_0$ is provided in Tables 1 and 2, respectively. For TGS 2611-C00 for example, a 1 ppm $[CH_4]$ enhancement above $[CH_4]_0$ corresponds to an RR change of -60 m$\Omega\ \Omega^{-1}$ given by eq 4, assuming [CO] to be fixed at $[CO]_0$.

Figure 3a,c,e confirms that eq 4 resolves to eq 1 on the bottom of the plots (when [CO] equals $[CO]_0$) for exclusive $[CH_4]$ variability and eq 2 on the left-hand side of the plots (when $[CH_4]$ equals $[CH_4]_0$) for exclusive [CO] variability, as expected, with small RR residuals. However, simultaneously high $[CH_4]$ and [CO] enhancements above reference levels (top right-hand corners in Figure 3a,c,e) cause slight RR underestimation compared to observations. This infers that the original CMM for methane and carbon monoxide overestimates TGS resistance decrease (i.e., predicted TGS resistance drop from R_0) when $[CH_4]$ and [CO] are simultaneously enhanced above their reference levels. This is supported by Table 3 mean bias errors, which show an overall negative RR bias when sampling mole fraction combinations during laboratory testing, for each TGS. We infer from this that other pairs of reducing gases may also exhibit an interdependence effect in the same way.

The RR underestimation observed during the laboratory tests presented here also has implications when using RR and [CO] to derive $[CH_4]$, by inverting eq 4 to make $[CH_4]$ the subject. The original CMM (eq 4) results in a predicted RR that is lower than measurements. Instead, using the higher measured RR to derive $[CH_4]$ similarly results in modeled $[CH_4]$ that is lower than actual $[CH_4]$ measurements (which correspond to a lower modeled eq 4 RR). To evaluate the importance of this $[CH_4]$ underestimation effect, 5 min averaged RR and [CO] values were treated as known model input and eq 4 was rearranged to make $[CH_4]$ the subject. Modeled $[CH_4]$ from eq 4 is compared to corresponding

https://doi.org/10.1021/acsomega.4c06397
ACS Omega XXXX, XXX, XXX−XXX

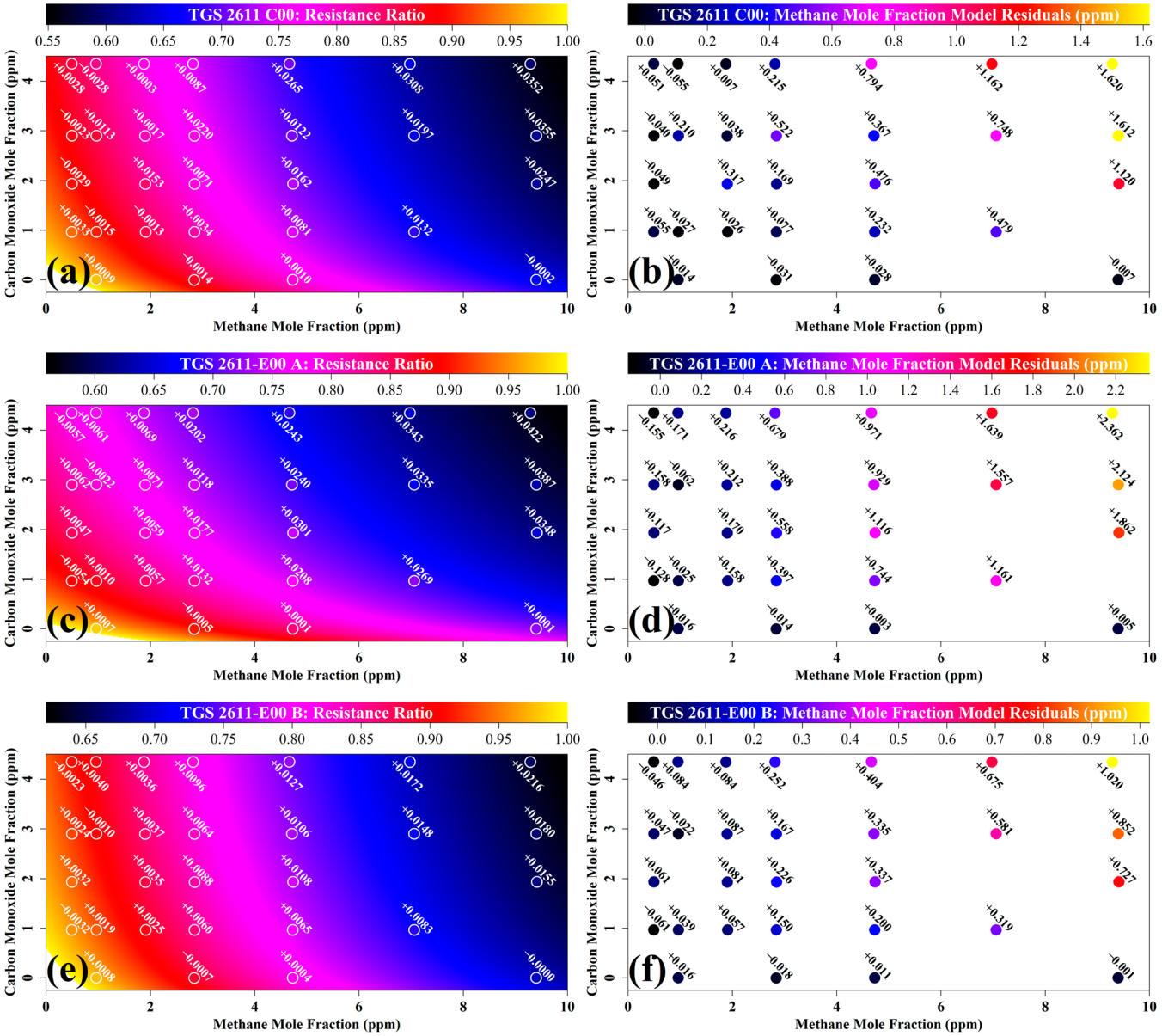

Figure 3. Equation 4 modeled RR as a function of 5 min average measured [CH_4] and [CO], plotted as a colored background in $\Omega\ \Omega^{-1}$ for (a) TGS 2611-C00, (c) TGS 2611-E00 A, and (e) TGS 2611-E00 B. 5 min average RR observations are shown as colored dots in white circles in (a), (c), and (e), with RR residuals also given. Residuals between measured [CH_4] and [CH_4] modeled by inverting eq 4 using corresponding 5 min average measured RR and [CO] are plotted for TGS 2611-C00 in (b), TGS 2611-E00 A in (d), and TGS 2611-E00 B in (f). Each panel has a unique color scale, where white represents RRs greater than one in (a), (c), and (e).

Table 3. RMSE, Correlation, and Mean Bias Error between Measured RR and RR Modeled with Eq 4 for Each TGS, Using *m*, *μ*, *n*, and *ν* Coefficients from Eqs 1 and 2[a]

sensor	Pearson correlation coefficient	RMSE ($m\Omega\ \Omega^{-1}$)	mean bias error ($m\Omega\ \Omega^{-1}$)	RMSE in derived [CH_4] (ppm)	mean bias error in derived [CH_4] (ppm)
TGS 2611-C00	1 − 0.00240	±15.3	−9.92	±0.593	−0.348
TGS 2611-E00 A	1 − 0.00336	±19.8	−13.90	±0.928	−0.599
TGS 2611-E00 B	1 − 0.00073	±9.1	−6.40	±0.363	−0.230

[a]Corresponding [CH_4] RMSE and mean bias error values are given when compared to measured [CH_4], by solving for [CH_4] in eq 4 using measured RR and [CO] as model input.

measured 5 min average [CH_4] from the reference gas analyzer in Figure 3b,d,f. Mean bias errors and RMSEs comparing modeled and measured [CH_4] are given in Table 3. Figure 3 shows that modeled [CH_4] underestimation using eq 4 may be important when [CH_4] and [CO] are simultaneously enhanced above their reference levels. Yet, the overall significance of this underestimation depends on model specificities, choice of reference gas, the nature of the individual TGS, and conditions during final sensor application. As an example for this specific test, a 4.3 ppm [CO]

https://doi.org/10.1021/acsomega.4c06397
ACS Omega XXXX, XXX, XXX−XXX

Table 4. Derived A, m, μ, n, and ν Coefficients from Eq 5 for Each TGS, with the RMSE in RR and the R^2 for Each Fit Given[a]

sensor	A (ppm^{-2})	m (ppm)	μ	n (ppm)	ν	RMSE ($m\Omega\ \Omega^{-1}$)	RMSE in derived $[CH_4]$ (ppm)	R^2
TGS 2611-C00	0.00178 ± 0.00029	10.2 ± 1.4	0.67 ± 0.07	0.8 ± 0.1	0.082 ± 0.008	±4.9	±0.147	0.99767
TGS 2611-E00 A	0.00207 ± 0.00029	15.6 ± 3.7	0.70 ± 0.14	0.7 ± 0.1	0.124 ± 0.008	±5.0	±0.217	0.99655
TGS 2611-E00 B	0.00091 ± 0.00010	12.7 ± 0.8	0.69 ± 0.04	1.0 ± 0.1	0.053 ± 0.003	±1.9	±0.055	0.99961

[a]Corresponding $[CH_4]$ RMSE values are given when compared to measured $[CH_4]$, by solving for $[CH_4]$ in eq 5 using measured RR and $[CO]$ as model inputs.

enhancement above $[CO]_0$ results in a −1.2 ppm $[CH_4]$ model underestimation at 7.0 ppm $[CH_4]$ (or −17% $[CH_4]$) for TGS 2611-C00. However, a 1.0 ppm $[CO]$ enhancement above $[CO]_0$ results in a far smaller −0.5 ppm $[CH_4]$ model underestimation at 7.1 ppm $[CH_4]$ (or −6.8% $[CH_4]$) for the same TGS. There are many practical field applications where −0.5 ppm $[CH_4]$ is an acceptable level of uncertainty bias. In general applications, the magnitude of any interdependence effect on derived mole fraction must be evaluated between the specific reducing gases in question and reference mole fraction levels, which can be different in different applications.

The outcome from this $[CH_4]$ and $[CO]$ study is that the original CMM underestimates RR in this case. This means that the original CMM underestimates $[CH_4]$ when eq 4 is inverted, using higher measured RR as input (as opposed to a lower RR corresponding to actual measured $[CH_4]$, according to the original CMM). This suggests that, in general, individual gases do not independently multiplicatively influence RR and that there may be some interdependence from different gas species. A single reducing gas on the SMO surface may change TGS sensitivity characteristics to another reducing gas. The physical cause of this phenomenon is beyond the scope of this empirical gas study. Nevertheless, we propose that this may be related to chemical SMO surface processes during methane and carbon monoxide oxidation; SMO surface kinetics are incredibly complex with several oxidation stages.[3,4,7] For example, some incomplete methane combustion can result in carbon monoxide as a waste product,[2] which may then subsequently compete for available surface absorption sites with fresh carbon monoxide in the original sample gas, possibly explaining an interdependence effect. More research is recommended on the physical cause of gas interdependence, such that any potential interdependence effects can be understood between other pairs of reducing gas species. In any case, it is surprising that this effect is observed at such low (trace ppm) mole fraction levels, where one would expect the molar density to be sufficiently low for independent sensor interaction, especially considering that both the TGS 2611-C00 and TGS 2611-E00 have otherwise been tested for sensitivity up to 10 000 ppm $[CH_4]$.[19,20]

3.4. Modified Combined Multiplicative Model. As the original Shah et al.[34] CMM may underestimate RR with simultaneously enhanced reducing gas mole fractions (compared to their reference levels), a modified model was devised, given by

$$R = R_0 \times \left(1 + \left(\frac{[CH_4] - [CH_4]_0}{m}\right)\right)^{-\mu} \times \left(1 + \left(\frac{[CO] - [CO]_0}{n}\right)\right)^{-\nu} \times \left(1 + \left(A \times \left(\left[CH_4\right] - \left[CH_4\right]_0\right) \times \left(\left[CO\right] - \left[CO\right]_0\right)\right)\right) \quad (5)$$

for the specific case of $[CH_4]$ and $[CO]$ enhancements. Equation 5 includes a methane and carbon monoxide interdependence coefficient (A), which is a very simple first-order correction term to combine the two gas mole fraction enhancements. This additional interdependence term elevates the original modeled RR closer to 1 through direct multiplication with the pre-existing terms in eq 4, when $[CH_4]$ and $[CO]$ are both enhanced above their reference gas levels. This also means that when either gas mole fraction is at its reference level, eq 5 simplifies to the original single gas equations (given by eq 1 for $[CH_4]$ and eq 2 for $[CO]$). If testing additional reducing gases (or a totally different set of reducing gases), a modified CMM could be formulated following eq 3 (as standard), alongside additional interdependence terms between each pair of reducing gases exhibiting an interdependence effect. Each interdependence effect would need to be identified and characterized. Therefore, a modified CMM with three reducing gases has up to three interdependence terms while a modified CMM with four reducing gases has up to six interdependence terms, following the series of triangular numbers between number of reducing gases and number of potential interdependence terms. Yet, the general assumptions presented here, on the behavior of interdependence effects on RR, are based only on interactions between methane and carbon monoxide, which is a limitation of this work.

In order to derive eq 5 coefficients for methane and carbon monoxide, two-dimensional $[CH_4]$ and $[CO]$ combinations are required. This is in contrast to the previous eq 1 and 2 analyses, which required variations in only single gas mole fractions. An NLS regression was thus applied using eq 5 between all 5 min average observed RR values and corresponding $[CH_4]$ and $[CO]$ from the reference gas analyzer, where original m, μ, n, and ν parameters from eqs 1 and 2 were used as starting values (i.e., a first guess and free to vary over subsequent iterations). This analysis yielded new m, μ, n, and ν values alongside A (see Table 4). Standard deviation uncertainty values are given in Table 4 for the newly derived coefficients, which were provided by R version 4.2.2[39] using rescaled covariances based on Hessian matrices.

https://doi.org/10.1021/acsomega.4c06397
ACS Omega XXXX, XXX, XXX−XXX

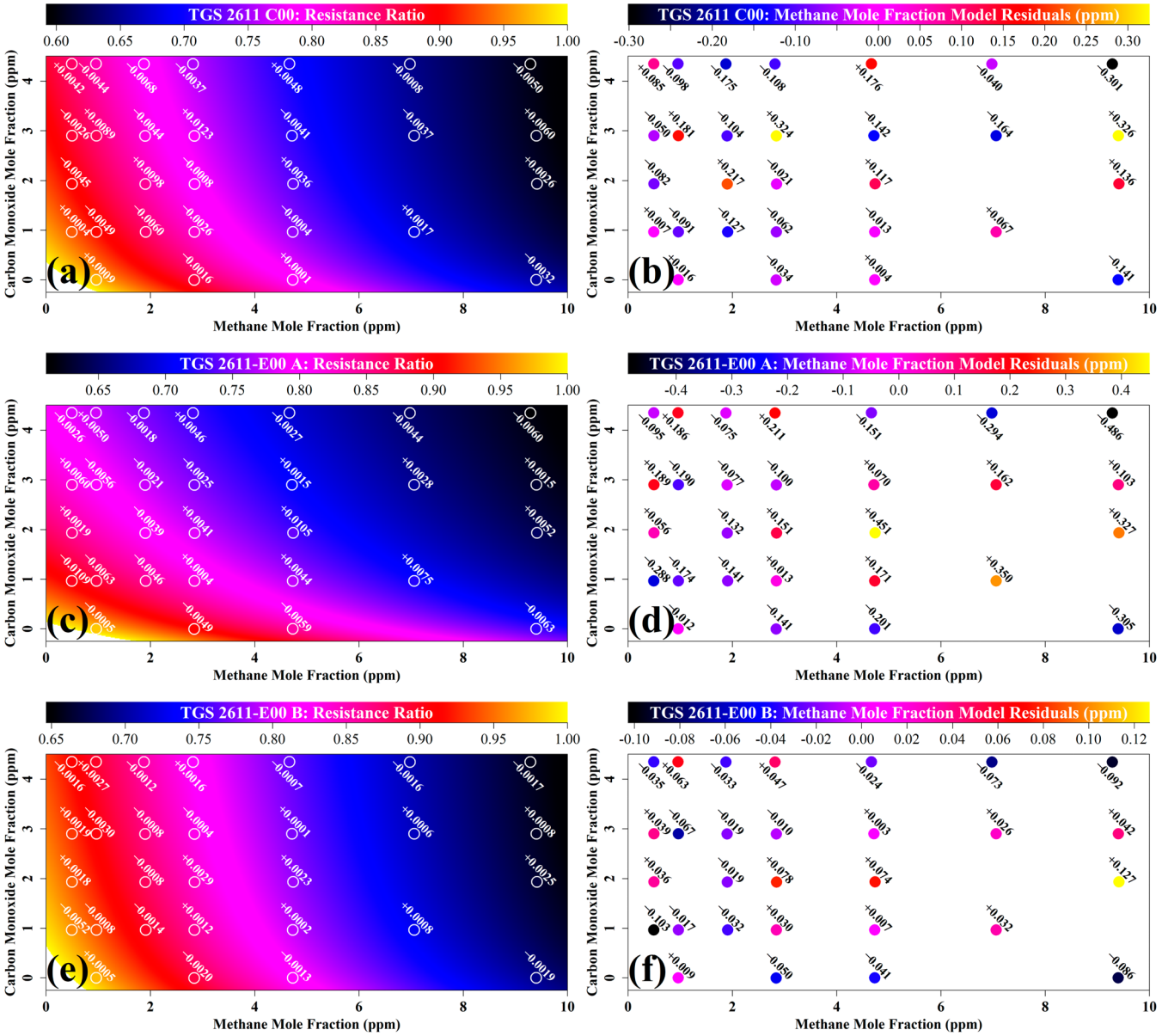

Figure 4. Equation 5 modeled RR as a function of 5 min average measured [CH_4] and [CO], plotted as a colored background in $\Omega\ \Omega^{-1}$ for (a) TGS 2611-C00, (c) TGS 2611-E00 A, and (e) TGS 2611-E00 B. 5 min average RR observations are shown as colored dots in white circles in (a), (c), and (e), with RR residuals also given. Residuals between measured [CH_4] and [CH_4] modeled by inverting eq 5 using corresponding 5 min average measured RR and [CO] are plotted for TGS 2611-C00 in (b), TGS 2611-E00 A in (d), and TGS 2611-E00 B in (f). Each panel has a unique color scale, where white represents RRs greater than one in (a), (c), and (e).

New m, μ, n, ν, and A coefficients could then be used to model corrected RRs as a function of corresponding 5 min average measured [CH_4] and [CO], for this methane and carbon monoxide test. Individual derived RR values from the modified CMM are compared to corresponding 5 min average RR observations in Figure 4a,c,e for each TGS. The RMSE between observed RR and corresponding modeled RR values from eq 5 is provided in Table 4 alongside the R^2 of each fit. Figure 4 demonstrates that the modified CMM can better replicate laboratory-observed RR than the original Shah et al.[34] CMM, using 5 min average [CH_4] and [CO] as sole model inputs. Crucially, RR model agreement is much improved when [CH_4] and [CO] are simultaneously enhanced above their reference levels (the top right-hand corner of each Figure 4a,c,e plot), in contrast to the original CMM (see Figure 3a,c,e).

RMSE RR values, which provide a metric of overall model constraint, are smaller for the modified CMM for methane and carbon monoxide (see Table 4) than when testing the original CMM (with m, μ, n, and ν derived from RR average subsets) against the full RR data set (given in Table 3). For example, the RMSE for TGS 2611-C00 reduces from $\pm$15.3 m$\Omega\ \Omega^{-1}$ for the original CMM to $\pm$4.9 m$\Omega\ \Omega^{-1}$ for the modified CMM. The validity and shape of the correction given by eq 5 is also evaluated by comparing new coefficients to original eq 1 and 2 coefficients in Section S2 of the Supporting Information. This shows that m and μ changed by no more than 20% compared to values from eq 1, whereas n and ν changed by no more than 40% compared to values from eq 2. Coefficients from eq 2

https://doi.org/10.1021/acsomega.4c06397
ACS Omega XXXX, XXX, XXX−XXX

were less constrained (i.e., they exhibited a larger variation compared to the new coefficients) than those from eq 1, which is hardly surprising considering its poorer fit with higher RMSEs. As an extra test, the same full two-dimensional [CH_4] and [CO] combination data set was used to derive new eq 4 coefficients in Section S3 of the Supporting Information. This analysis was conducted to confirm that the use of eq 5 was the true cause in improved RR RMSE values, as opposed to potential issues in coefficients from original eq 1 and 2 fits when applied to full testing data set. As a final test, the justification for added constraint from the eq 5 A parameter was confirmed by conducing Akaike information criterion (AIC) and Bayesian information criterion (BIC) tests by using eq 5 as opposed to eq 4, when applied to the full two-dimensional RR data set, which are presented in Section S4 in the Supporting Information. Thus, the simple inclusion of an A gas interdependence term in the original CMM considerably improves RR estimation from multiple raw measured [CH_4] and [CO] levels, simultaneously enhanced above their reference levels.

Next, as for the original CMM, it is useful here to evaluate the influence on [CH_4] derivation from RR using this modified CMM. This was achieved using all observed 5 min averaged measured RRs and measured [CO] values as eq 5 input. [CH_4] was derived by minimizing the squared residuals between observed and modeled RR through gradual [CH_4] adjustments, as eq 5 has no analytical [CH_4] solution. These new modeled [CH_4] values are compared to measured 5 min averages made by the reference gas analyzer in Figure 4. RMSEs using the modified CMM given by eq 5 are provided in Table 4, compared to corresponding 5 min average measurements made by the reference gas analyzer. Figure 4b,d,f [CH_4] residuals are clearly smaller than corresponding Figure 3 values. In addition, derived [CH_4] RMSE is much improved; for example, it reduces from ±0.593 ppm for the original CMM for TGS 2611-C00 to ±0.147 ppm for the modified CMM (see values in Tables 3 and 4). This shows that the modified CMM provides better overall constraint and thus better [CH_4] estimation from RR, when sampling simultaneous multiple reducing gas enhancements.

Finally, the improvement in modified CMM [CH_4] estimation from RR and [CO] can be evaluated across a continuous [CH_4] and [CO] range (up to 10 and 5 ppm tested here, respectively), compared to the original CMM. A continuous RR was obtained using eq 5 with derived m, μ, n, ν, and A. Then, the original CMM was used to derive [CH_4] from these RR values and corresponding [CO] measurements, by inverting eq 4 to make [CH_4] the subject. This analysis fundamentally assumes eq 5 to provide an accurate representation of laboratory RR observations as a function of [CH_4] and [CO]. This is a reasonable assumption, considering relatively low RR RMSEs from the modified CMM (see Table 4).

Residuals between [CH_4] predicted by the original CMM compared to [CH_4] used as eq 5 input (to derive expected RR) are shown in Figure 5. This is analogous to Figure 3b,d,f plots, supporting the previously discussed conclusions of eq 4 [CH_4] underestimation, but with Figure 5 not being limited to discrete [CH_4] and [CO] laboratory sampling points. For the TGS 2611-C00, for example, a 6 ppm [CH_4] level and 0.1 ppm [CO] level results in [CH_4] underestimation of 0.0959 ppm (or −1.60% [CH_4]), assuming a $[CH_4]_0$ of 0.492 ppm and a $[CO]_0$ of 0 ppm. However, a 6 ppm [CH_4] level and 1 ppm

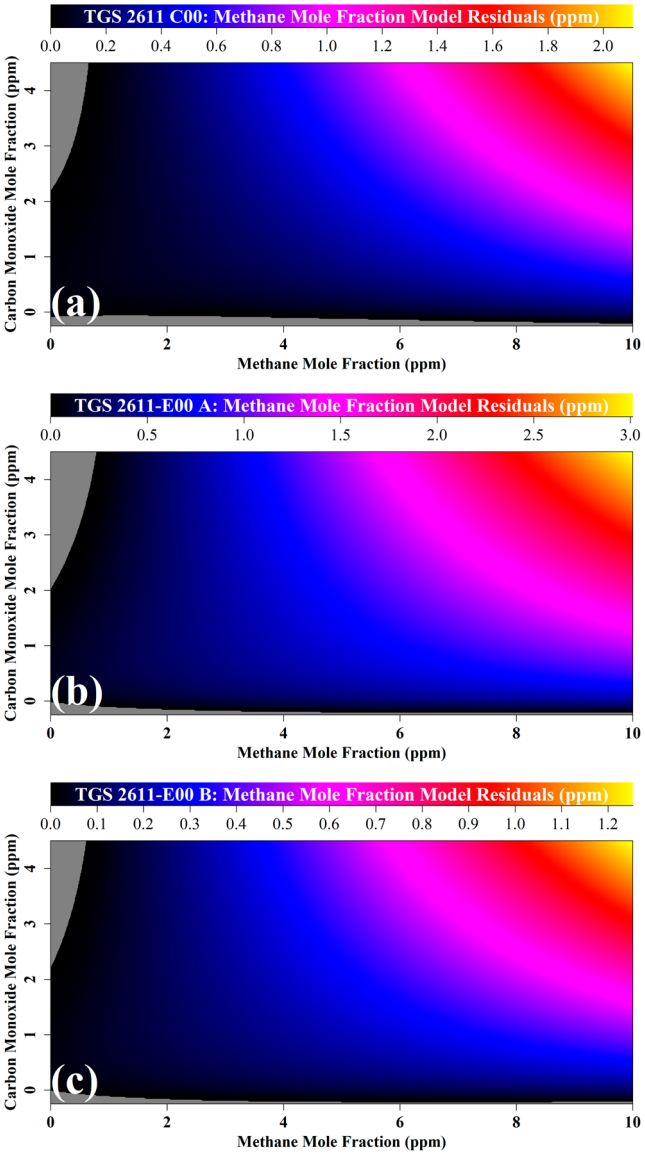

Figure 5. Difference between [CH_4] used as input to derive an RR using the modified CMM given by eq 5 and [CH_4] derived from corresponding RR using the original CMM given by eq 4, plotted as colored dots in ppm for (a) TGS 2611-C00, (b) TGS 2611-E00 A, and (c) TGS 2611-E00 B. Each plot has a unique sensor-specific color scale. Residuals of a [CH_4] of less than 0 ppm are plotted in gray.

[CO] level results in a much larger eq 4 [CH_4] underestimation of 0.341 ppm (or −5.68% [CH_4]). Thus, this work emphasizes the importance of accurately identifying and incorporating interdependence effects within a specific model when using TGS RR to predict gas mole fractions in complex gas mixtures.

4. DISCUSSION

Reducing gases, such as those detected by TGSs, require atmospheric observations for a multitude of reasons, depending on the reducing gas in question. For example, hydrogen is extremely flammable, which can pose safety concerns, especially with its increasing use as an end-use fuel. Carbon monoxide is a reducing gas that can cause health issues when respired. Methane is a potent greenhouse gas leading to global warming with many natural and anthropogenic sources. It is

https://doi.org/10.1021/acsomega.4c06397
ACS Omega XXXX, XXX, XXX−XXX

therefore essential to understand how the TGS behaves when simultaneously exposed to more than one reducing gas such that a suitable mole fraction model can be derived from RR in complex environments. The importance of any variations in the reference gas composition must also be evaluated when deriving mole fractions for a single reducing gas. Therefore, in this study, we characterized the RR effect of simultaneous [CH_4] and [CO] enhancements (with these two gas mole fractions serving as an example), to better understand the potential importance of interdependence effects when modeling TGS response to multiple reducing gases, simultaneously enhanced in mole fraction.

We confirm that the Shah et al.[34] gas characterization model applies to both methane and carbon monoxide individually. This is reflected in an R^2 of at least 0.9 for individual [CH_4] and [CO] fits (see Tables 1 and 2, respectively). However, this work also exhibits limitations in the original Shah et al.[34] CMM (generalized by eq 3 for multiple reducing gases), when [CH_4] and [CO] are simultaneously enhanced, compared to their specific predefined reference gas levels. This is because the original CMM assumes the RR change due to one target gas species to be independent of the RR effect of all other reducing gas species. In reality, laboratory testing for simultaneous [CH_4] and [CO] enhancements showed modeled RRs (derived using eq 4) to be slightly lower than corresponding observed values (see Figure 3a,c,e). This is therefore indicative of an interdependence effect due to cross-sensitivities between the two reducing gases tested in this work, lowering their combined effect on RR (i.e., increasing net RR closer to one).

We provide an extension to the original CMM to account for this interdependence effect, by proposing a modified CMM for gas characterization. This is given by eq 5 for [CH_4] and [CO] enhancements, as tested in this study, which provides a better representation of observed RR. The improvements of this modified CMM are emphasized in Figure 5 when using RR to estimate [CH_4], where [CH_4] is corrected by −1.9 ppm for the TGS 2611-C00, at 10 ppm [CH_4] and 4 ppm [CO] (assuming a $[CH_4]_0$ of 0.492 ppm and a $[CO]_0$ of 0 ppm). It is important to state that interdependence effects have only been characterized for two specific reducing gases in this work. Other reducing gases may also cause RR disparity, which could also be resolved by including interdependence terms within a modified CMM. However, it is possible that a specific pair of reducing gases exhibits no interdependence effects, which would need to be assessed for each pair of reducing gases, if necessary. In a case with more than two variable reducing gases, we propose that each interdependence term between each reducing gas and each other reducing gas could simply be included multiplicatively within a modified CMM, although this needs to be confirmed in future work. It is also important to note that eq 5 uses a relatively basic first-order correction term. This was chosen as there were insufficient sampling points across the existing [CH_4] and [CO] space to explore a more complex correction (e.g., a power fit). Additional future characterization tests may yield a better understanding of interdependence effects. However, with the low cost and targeted accuracy of SMO sensors, testing to further improve the proposed modified CMM may be unfeasible and unnecessary, considering the associated effort for minimal improvement in RR characterization as a function of interdependent gas response. Thus, the basic modified CMM for gas characterization (given by eq 5) for [CH_4] and [CO] variability) is typically sufficient, serving as a useful contribution to improve reducing gas mole fraction measurement using TGS sampling.

This work (along with a previous study[32]) confirms that the Shah et al.[34] gas characterization model applies to single reducing gases. However, this fit has never been tested for oxidizing gases. It is presumed that the power in such a fit would be preceded by a positive sign for an individual oxidizing gas, leading to an RR of greater than 1. In the presence of multiple gas enhancements, an oxidizing gas term would simply be included in the original CMM (eq 3) as an additional multiplicative term with a positive signed power, alongside reducing gas terms with negative signs preceding each power. We presume that interdependence correction terms within a modified CMM may either use a positive or negative interdependence term, depending on the specificities of the interaction (if any) between the oxidizing gas in question and each other reducing gas. This would need to be tested in future work for confirmation (if relevant) depending on the sampling environment. However, the oxidative capacity of Earth's atmosphere is usually relatively stable, with molecular oxygen as the main oxidizing gas in the atmosphere. Most reducing gas emissions either occur alone or alongside emissions of other reducing gases and not alongside oxidizing gases (such as chlorine or ozone, for example).

A key outcome from this specific work on methane and carbon monoxide is that each TGS requires a unique set of m, μ, n, ν, and A values, even sensors of the same type, as each coefficient for the three TGS units is different (see Tables 1, 2, and 4), confirming previous observations.[6,22,25,27,34] This is supported by different R_0 values for each sensor, as shown in Figure 1, despite the fact that each TGS sampled the same reference gas. Yet, regardless of individual differences, each TGS adhered to the overall modified RR CMM for methane and carbon monoxide given by eq 5. Thus, the original CMM for gas characterization can be rectified in the same way, with a simple first-order multiplicative interdependence correction term, for both TGS types in this study, provided that adequate testing is conducted on each unique sensor.

The key utility of any RR model in a field application is to invert the model to yield an unknown gas mole fraction from measured RR.[33] Yet, for the example of measuring [CH_4] with carbon monoxide interference, the use of eq 5 (the modified CMM) is more difficult than eq 4 (the original CMM), as [CH_4] cannot be solved analytically from eq 5. In addition, both the modified CMM (which includes gas interdependence) and the original CMM (without gas interdependence) only allow derivation of a single unknown gas mole fraction. This requires a measurement of all other reducing gas mole fractions enhanced above their reference gas levels. For example, as discussed in Section 1, if deriving [CH_4] where ethane or carbon monoxide emissions also occur, then a separate ethane mole fraction ([C_2H_6]) or [CO] measurement, respectively, would be required.

Yet there are many applications where only a single reducing gas mole fraction can be assumed to vary, thus simplifying gas characterization models. As well as absolving the need for mole fraction measurements of all other reducing gases, this can also avoid the time-consuming task of calculating individual interdependent gas correction terms between each varying reducing gas; for this specific work (only two interdependent gases), A required at least one full day of laboratory testing. Instead, each individual TGS only needs to be characterized in

https://doi.org/10.1021/acsomega.4c06397
ACS Omega XXXX, XXX, XXX−XXX

response to a single reducing gas species. For the example of measuring [CH_4] with carbon monoxide interference, $[CO]_0$ can be set to any level, as $[CO]_0$ is defined according to [CO] during methane characterization testing. $[CO]_0$ may logically be assigned to the ambient background level as for both eqs 4 and 5, when [CO] equals $[CO]_0$ (i.e., assuming constant [CO] of $[CO]_0$ in the field), then both equations resolve to eq 1, which is independent of [CO]. This principle was applied by Shah et al.[32] who measured TGS [CH_4] at a landfill site, where [CO] was assumed to be fixed at its ambient background level. However, constant [CO] (at $[CO]_0$) was only an assumption and [CO] inevitably varied from $[CO]_0$ during ambient sampling, thereby influencing RR alongside [CH_4]. This can result in an additional uncertainty on [CH_4] estimates, which was deemed to be insignificant in the Shah et al.[32] study, with dominant [CH_4] variability. Nevertheless, in general, the additional uncertainty incurred by a naturally variable background composition assumed to be constant must be adjudged to be sufficiently small relative to the required accuracy of the final application.

A key implication of the modified CMM on TGS response is the requirement for gas characterization terms to be derived using a reference gas with an identical composition to the field sampling gas, except for explicitly characterized reducing gases. Otherwise (noncharacterized) interdependent gas terms will not cancel out in RR causing differences in the nature of the gas characterization fit. This general requirement applies when both using the original CMM generalized by eq 3 (for either a single or multiple gases) as well as if introducing gas interdependence terms within this model (for multiple gases). To make sense of this, for example, measuring [CH_4] with carbon monoxide, based on the original understanding of eq 4, when [CO] is equal to any fixed value, the carbon monoxide multiplicative term is a constant regardless of [CH_4]. This allows m and μ to be derived with any constant [CO] setting as the same fixed multiplicative constant will be present when sampling $[CH_4]_0$ (i.e., the reference gas representing R_0) as well as when sampling [CH_4] greater than $[CH_4]_0$, therefore canceling out in an RR. However, according to eq 5, when [CO] is not equal to $[CO]_0$, the interdependence term is not constant and varies with [CH_4]. Therefore, a universal set of m and μ values cannot be derived at any [CO] level and [CO] must be defined as being equal to $[CO]_0$ during any RR methane characterization testing. This general requirement for interfering gases to be at their reference levels during gas characterization may explain why gas characterization coefficients derived in synthetic air are different to those derived in ambient air,[32] with Shah et al.[34] showing that interfering reducing species may be naturally present in ambient air. These potential ambient interfering species may have a methane interdependence effect.

This oversight in reference gas characterization conditions occurred in the Shah et al.[32] landfill study, where methane characterization was conducted at a [CO] of 0 ppm, while $[CO]_0$ was assumed to be at an ambient (nonzero) background level in the field. This inevitably led to a suboptimal methane characterization RR fit, due to carbon monoxide absence. In hindsight, Shah et al.[32] should have either derived A (to postcorrect for methane and carbon monoxide interdependence at a fixed ambient [CO] level) or derived methane coefficients in a reference gas containing an ambient [CO] level, with the latter being the simpler option. Yet, based on the disparity induced in this study by using the original CMM instead of the modified CMM shown in Figure 5, an ambient [CO] field enhancement (approximately 0.1 ppm) above the 0 ppm reference level during gas characterization in that study was unlikely to be too significant on m and μ methane coefficients. Furthermore, Shah et al.[32] successfully targeted a [CH_4] accuracy of ±1 ppm, which was verified using a reference instrument, making m and μ derived assuming validity of the original Shah et al.[34] CMM to be a reasonable approximation in that study.

In summary, the findings from this work have a minor influence on the Shah et al.[32] landfill study to derive [CH_4], which was a special case in ideal conditions. The influence of carbon monoxide interdependence on methane fitting coefficients was expected to be small due to minor ambient [CO] field enhancements compared to the 0 ppm [CO] present during laboratory testing. Yet, this does not reflect best practice and future work should either postcorrect for [CO] interdependence or conduct methane characterization at an appropriate $[CO]_0$ level, as discussed above. In addition, the Shah et al.[32] landfill study assumed that [CO] did not vary from its ambient level, due to absence of major carbon monoxide sources. This would be an unsuitable approach to measure [CH_4] in the vicinity of fires or vehicular emissions (i.e., near roads), which can result in [CO] being consistently elevated above the ambient background. This effect could either be corrected with methane characterization testing at an elevated [CO] level (for interdependence effects to cancel in the methane characterization RR) or with methane and carbon monoxide interdependence characterization for postcorrection. If [CO] variation is expected, this would also need to be accounted for using a separate [CO] measurement, where a judgment would need to be made on whether to include interdependence effects, depending on accuracy requirements. Similarly, a gas extraction site may also pose problems in TGS [CH_4] or [C_2H_6] measurements due to simultaneous emissions of both gases. Interdependence effects may be vital for improved accuracy. A separate measurement of either [C_2H_6] or [CH_4] would also be needed as only one unknown gas can be derived. Thus, this work emphasizes the importance of either conducting gas characterization with suitable background levels of other reducing gases (even if ignoring interdependence effects and applying the original CMM as an approximation) or by characterizing the interdependence effect between each pair of reducing gases expected to diverge in the field compared to their defined reference levels during laboratory testing.

5. CONCLUSIONS

The resistance of SMO sensors is influenced by reducing gases; this is the principle for retrieving gas mole fraction levels in field applications. The ratio between sensor resistance with enhanced reducing gas levels (the numerator) compared to resistance with reference reducing gas levels (the denominator) can be modeled as a function of reducing gas mole fractions. This RR removes the effect of (non-reducing gas mole fraction) environmental conditions as a first step, allowing for independent analysis of TGS reducing gas response. A robust characterization and understanding of the response of sensors, such as the TGS, to reducing gas mixtures is essential for their informed deployment when sampling the ambient atmosphere. To evaluate the influence of different reducing gases on RR, we tested one TGS 2611-C00 and two TGS 2611-E00 units under exposure to different [CH_4] and [CO] combinations, in a

https://doi.org/10.1021/acsomega.4c06397
ACS Omega XXXX, XXX, XXX−XXX

controlled laboratory experiment. [CH_4] was varied between 0.5 and 9.4 ppm, and [CO] was varied between 0 and 4.3 ppm. Each reducing gas was hypothesized to effect net RR independently of all other reducing gases. We found this original assumption to be a valuable approximation in certain gas mixtures. However, some RR model disparity was observed during simultaneously high [CH_4] and [CO] enhancements. Although this study only characterized interdependence effects between two specific gases, we infer from this that similar interdependence effects may be observed between any other two reducing gases, whereby each gas in the mixture may influence the effect of every other reducing gas on net RR. This means that TGS RR may not decrease by as much as it would do if each reducing gas independently influenced RR. The general presence of interdependence effects is not an issue if using TGS sampling to derive single gas mole fractions. However, this nevertheless requires the reference gas during gas characterization to be identical to gas during final sensor deployment, for residual background interdependence effects to cancel; this is in contrast to testing requirements inferred from our original understanding of TGS response to multiple gases, which allowed for any reference gas mixture during RR characterization of a single reducing gas. If using TGS sampling to observe multiple reducing gas enhancements (for example, to measure [CH_4] in a wetland area with variable [CO] due to fires), we propose a simple correction to improve the original gas characterization model by including an interdependent gas characterization term. In theory, the same principle can be applied in more complex environments where more than two reducing gases are enhanced in mole fraction (compared to reference levels), by simply including interdependence terms between each reducing gas and each other reducing gas within an RR model, although the presence and nature of all such effects should be tested in future work if necessary. The reason for this reducing gas interdependence effect (observed here between methane and carbon monoxide) is not clear, but it may be due to semiconductor surface interactions between multiple reducing gases. In any case, this work provides a useful understanding of the potential complications of using TGS sampling to measure mole fraction enhancements from multiple reducing gases. It also allows us to conclude that TGS sampling may be more suited to measure the mole fraction of a single reducing gas.

■ ASSOCIATED CONTENT

Supporting Information

The Supporting Information is available free of charge at https://pubs.acs.org/doi/10.1021/acsomega.4c06397.

(S1) Logging system; (S2) change in original coefficients; (S3) original combined multiplicative model coefficients from the full data set; and (S4) parameterization of interdependence coefficient (PDF)

■ AUTHOR INFORMATION

Corresponding Author

Adil Shah − *Laboratoire des Sciences du Climat et de l'Environnement (CEA-CNRS-UVSQ), Institut Pierre-Simon Laplace, Université Paris-Saclay, Gif-sur-Yvette 91191, France*; orcid.org/0000-0002-5692-3715; Email: adil.shah@lsce.ipsl.fr

Authors

Olivier Laurent − *Laboratoire des Sciences du Climat et de l'Environnement (CEA-CNRS-UVSQ), Institut Pierre-Simon Laplace, Université Paris-Saclay, Gif-sur-Yvette 91191, France*

Grégoire Broquet − *Laboratoire des Sciences du Climat et de l'Environnement (CEA-CNRS-UVSQ), Institut Pierre-Simon Laplace, Université Paris-Saclay, Gif-sur-Yvette 91191, France*; orcid.org/0000-0001-7447-6907

Pramod Kumar − *Laboratoire des Sciences du Climat et de l'Environnement (CEA-CNRS-UVSQ), Institut Pierre-Simon Laplace, Université Paris-Saclay, Gif-sur-Yvette 91191, France*

Philippe Ciais − *Laboratoire des Sciences du Climat et de l'Environnement (CEA-CNRS-UVSQ), Institut Pierre-Simon Laplace, Université Paris-Saclay, Gif-sur-Yvette 91191, France*

Complete contact information is available at: https://pubs.acs.org/10.1021/acsomega.4c06397

Author Contributions

A.S.: conceptualization, methodology, formal analysis, investigation, and writing—original draft; O.L.: resources, writing—review and editing, and project administration; G.B.: conceptualization and writing—review and editing; P.K.: writing—review and editing; and P.C.: writing—review and editing, project administration, and funding acquisition.

Notes

The authors declare no competing financial interest.

■ ACKNOWLEDGMENTS

This work received funding from the Integrated Carbon Observation System (ICOS) National Network France. This work also received contributions in kind from SUEZ and the Chaire Industrielle TRACE, which is cofunded by the Agence Nationale de la Recherche (ANR) French National Research Agency (grant number: ANR-17-CHIN-0004-01), SUEZ, TotalEnergies - OneTech, and Thales Alenia Space.

■ REFERENCES

(1) Hodgkinson, J.; Tatam, R. P. Optical gas sensing: a review. *Measurement Science and Technology* **2013**, *24*, No. 012004.

(2) Kohl, D. Surface processes in the detection of reducing gases with SnO2-based devices. *Sens. Actuators* **1989**, *18*, 71−113.

(3) Bărsan, N.; Ionescu, R.; Vancu, A. Calibration curve for SnO2-based sensors. *Sens. Actuators, B* **1994**, *19*, 466−469.

(4) Kohl, D. The role of noble metals in the chemistry of solid-state gas sensors. *Sens. Actuators, B* **1990**, *1*, 158−165.

(5) Barsan, N.; Koziej, D.; Weimar, U. Metal oxide-based gas sensor research: How to? *Sens. Actuators, B* **2007**, *121*, 18−35.

(6) Clifford, P. K.; Tuma, D. T. Characteristics of semiconductor gas sensors I. *Steady state gas response, Sensors and Actuators* **1982**, *3*, 233−254.

(7) Kohl, D. Function and applications of gas sensors. *J. Phys. D: Appl. Phys.* **2001**, *34*, R125−R149.

(8) Suto, H.; Inoue, G. A New Portable Instrument for In Situ Measurement of Atmospheric Methane Mole Fraction by Applying an Improved Tin Dioxide−Based Gas Sensor. *Journal of Atmospheric and Oceanic Technology* **2010**, *27*, 1175−1184.

(9) Spinelle, L.; Gerboles, M.; Kok, G.; Persijn, S.; Sauerwald, T. Review of Portable and Low-Cost Sensors for the Ambient Air Monitoring of Benzene and Other Volatile Organic Compounds. *Sensors* **2017**, *17*, 1520.

(10) Kooti, M.; Keshtkar, S.; Askarieh, M.; Rashidi, A. Progress toward a novel methane gas sensor based on SnO2 nanorods-nanoporous graphene hybrid. *Sens. Actuators, B* **2019**, *281*, 96−106.
(11) Moalaghi, M.; Gharesi, M.; Ranjkesh, A.; Hossein-Babae, F. Tin oxide gas sensor on tin oxide microheater for high-temperature methane sensing. *Mater. Lett.* **2020**, *263*, No. 127196.
(12) Lin, J. J. Y.; Buehler, C.; Datta, A.; Gentner, D. R.; Koehler, K.; Zamora, M. L. Laboratory and field evaluation of a low-cost methane sensor and key environmental factors for sensor calibration. *Environmental Science: Atmospheres* **2023**, *3*, 683−694.
(13) Mills, I.; Cvitaš, T.; Homann, K.; Kallay, N.; Huchitsu, K. General Chemistry In *Quantities, Units and Symbols in Physical Chemistry*, 2nd ed., Blackwell Science Ltd.: Oxford, United Kingdom, 1993, pp.41−47.
(14) Wang, C.; Yin, L.; Zhang, L.; Xiang, D.; Gao, R. Metal Oxide Gas Sensors: Sensitivity and Influencing Factors. *Sensors* **2010**, *10*, 2088−2106.
(15) Haridas, D.; Gupta, V. Study of collective efforts of catalytic activity and photoactivation to enhance room temperature response of SnO2 thin film sensor for methane. *Sens. Actuators, B* **2013**, *182*, 741−746.
(16) Navazani, S.; Hassanisadi, M.; Eskandari, M. M.; Talaei, Z. Design and evaluation of SnO2-Pt/MWCNTs hybrid system as room temperature-methane sensor. *Synth. Met.* **2020**, *260*, No. 116267.
(17) Eugster, W.; Laundre, J.; Eugster, J.; Kling, G. W. Long-term reliability of the Figaro TGS 2600 solid-state methane sensor under low-Arctic conditions at Toolik Lake. *Alaska, Atmospheric Measurement Techniques* **2020**, *13*, 2681−2695.
(18) Eugster, W.; Kling, G. W. Performance of a low-cost methane sensor for ambient concentration measurements in preliminary studies. *Atmospheric Measurement Techniques* **2012**, *5*, 1925−1934.
(19) Figaro Engineering Inc., *TGS 2611-C00 - for the detection of Methane* tgs2611-c00_product information(fusa)rev01.pdf, 2022, https://www.figarosensor.com/product/docs/tgs2611-c00_product%20information%28fusa%29rev01.pdf.
(20) Figaro Engineering Inc.. *TGS 2611-E00 - for the detection of Methane* tgs2611-e00_product_information(fusa)_rev02.pdf, 2022, https://www.figarosensor.com/product/docs/tgs2611-e00_product_information%28fusa%29_rev02.pdf.
(21) Riddick, S. N.; Mauzerall, D. L.; Celia, M.; Allen, G.; Pitt, J.; Kang, M.; Riddick, J. C. The calibration and deployment of a low-cost methane sensor. *Atmos. Environ.* **2020**, *230*, No. 117440.
(22) Domènech-Gil, G.; Duc, N. T.; Wikner, J. J.; Eriksson, J.; Påledal, S. N.; Puglisi, D.; Bastviken, D. Electronic Nose for Improved Environmental Methane Monitoring. *Environ. Sci. Technol.* **2024**, *58*, 352−361.
(23) Yang, B.; Zhang, Z.; Tian, C.; Yuan, W.; Hua, Z.; Fan, S.; Wu, X.; Tian, X. Selective detection of methane by HZSM-5 zeolite/Pd-SnO2 gas sensors. *Sens. Actuators, B* **2020**, *321*, No. 128567.
(24) Bastviken, D.; Nygren, J.; Schenk, J.; Parellada Massana, R.; Duc, N. T. Technical note: Facilitating the use of low-cost methane (CH4) sensors in flux chambers - calibration, data processing, and an open-source make-it-yourself logger. *Biogeosciences* **2020**, *17*, 3659−3667.
(25) Cho, Y.; Smits, K. M.; Riddick, S. N.; Zimmerle, D. J. Calibration and field deployment of low-cost sensor network to monitor underground pipeline leakage. *Sens. Actuators, B* **2022**, *355*, No. 131276.
(26) Furuta, D.; Sayahi, T.; Li, J.; Wilson, B.; Presto, A. A.; Li, J. Characterization of inexpensive metal oxide sensor performance for trace methane detection. *Atmospheric Measurement Techniques* **2022**, *15*, 5117−5128.
(27) Riddick, S. N.; Ancona, R.; Cheptonui, F.; Bell, C. S.; Duggan, A.; Bennett, K. E.; Zimmerle, D. J. A cautionary report of calculating methane emissions using low-cost fence-line sensors. *Elementa* **2022**, *10*, No. 00021.
(28) Wu, Z.; Zhang, H.; Sun, W.; Lu, N.; Yan, M.; Wu, Y.; Hua, Z.; Fan, S. Development of a Low-Cost Portable Electronic Nose for Cigarette Brands Identification. *Sensors* **2020**, *20*, 4239.
(29) Rivera Martinez, R.; Santaren, D.; Laurent, O.; Cropley, F.; Mallet, C.; Ramonet, M.; Caldow, C.; Rivier, L.; Broquet, G.; Bouchet, C.; Juery, C.; Ciais, P. The Potential of Low-Cost Tin-Oxide Sensors Combined with Machine Learning for Estimating Atmospheric CH4 Variations around Background Concentration. *Atmosphere* **2021**, *12*, 107.
(30) Rivera Martinez, R. A.; Santaren, D.; Laurent, O.; Broquet, G.; Cropley, F.; Mallet, C.; Ramonet, M.; Shah, A.; Rivier, L.; Bouchet, C.; Juery, C.; Duclaux, O.; Ciais, P. Reconstruction of high-frequency methane atmospheric concentration peaks from measurements using metal oxide low-cost sensors. *Atmospheric Measurement Techniques* **2023**, *16*, 2209−2235.
(31) Butturini, A.; Fonollosa, J. Use of metal oxide semiconductor sensors to measure methane in aquatic ecosystems in the presence of cross-interfering compounds. *Limnology and Oceanography* **2022**, *20*, 710−720.
(32) Shah, A.; Laurent, O.; Broquet, G.; Philippon, C.; Allegrini, E.; Kumar, P.; Ciais, P. Determining methane mole fraction at a landfill site using the Figaro Taguchi gas sensor 2611-C00 and wind direction measurements. *Environmental Sciences Atmospheres* **2024**, *4*, 362−386.
(33) Jørgensen, C. J.; Mønster, J.; Fuglsang, K.; Christiansen, J. R. Continuous methane concentration measurements at the Greenland ice sheet−atmosphere interface using a low-cost, low-power metal oxide sensor system. *Atmos. Meas. Tech.* **2020**, *13*, 3319−3328.
(34) Shah, A.; Laurent, O.; Lienhardt, L.; Broquet, G.; Rivera Martinez, R.; Allegrini, E.; Ciais, P. Characterising the methane gas and environmental response of the Figaro Taguchi Gas Sensor (TGS) 2611-E00. *Atmospheric Measurement Techniques* **2023**, *16*, 3391−3419.
(35) Duan, Z.; Scheutz, C.; Kjeldsen, P. Trace gas emissions from municipal solid waste landfills: A review. *Waste Manage.* **2021**, *119*, 39−62.
(36) Rivera Martinez, R.; Kumar, P.; Laurent, O.; Broquet, G.; Caldow, F. C.; Cropley; Santaren, D.; Shah, A.; Mallet, C.; Ramonet, M.; Rivier, L.; Juery, C.; Duclaux, O.; Bouchet, C.; Allegrini, E.; Utard, H.; Ciais, P. Using metal oxide gas sensors for the estimate of methane controlled releases: reconstruction of the methane mole fraction time-series and quantification of the release rates and locations. *Atmospheric Measurement Techniques* **2024**, *17*, 4257−4290.
(37) Picarro, Inc.. *G2401 Analyzer Datasheet* | Picarro, 2021, https://gas.picarro.com/sites/default/files/product_documents/Picarro_G2401%20Datasheet_211029.pdf.
(38) van den Bossche, M.; Rose, N. T.; De Wekker, S. F. J. Potential of a low-cost gas sensor for atmospheric methane monitoring. *Sens. Actuators, B* **2017**, *238*, 501−509.
(39) R Core Team. *R: The R Project for Statistical Computing*, 2022, https://www.r-project.org/.

https://doi.org/10.1021/acsomega.4c06397
ACS Omega XXXX, XXX, XXX−XXX